

## Original Article

# Ultrasonographic features and inflammatory status associated with tumor size in breast invasive ductal carcinoma

Xiao-Hong Liu, Mei-Zhen Fan, Lin Lin, Ying-Ying Bai, Miao Zhang

Department of Ultrasound, The Affiliated Hospital of Bei-Hua University, Jilin 132000, Jilin, China

Received June 20, 2025; Accepted December 10, 2025; Epub January 15, 2026; Published January 30, 2026

**Abstract:** Objectives: This study explored how ultrasound features relate to tumor size and inflammatory markers in invasive ductal carcinoma (IDC) patients. Methods: We retrospectively reviewed 218 female IDC patients. Based on the largest diameter of the tumor, patients were split into two groups: those with tumors  $\leq 2$  cm and those with tumors  $> 2$  cm. We gathered data from conventional ultrasound (CUS), contrast-enhanced ultrasound (CEUS), and virtual touch tissue imaging quantification (VTIQ), along with blood-based inflammation indicators like neutrophil count and C-reactive protein (CRP) levels. Group comparisons were done using univariate analysis, and Spearman correlation was used to examine relationships between tumor size and other variables. Results: Larger tumors were more frequently located in the upper outer quadrant (60.71% vs 41.03%,  $P = 0.035$ ) and showed richer blood flow (73.57% vs 53.85%,  $P = 0.003$ ). By CEUS, larger tumors were more likely to show high enhancement (90% vs 78.21%,  $P = 0.017$ ) and expanded enhancement range (82.86% vs 70.51%,  $P = 0.034$ ). VTIQ results showed that SWV max ( $P = 0.033$ ), SWV peritumoral average (peri-avg) ( $P = 0.010$ ), and SWVR max/min ( $P = 0.009$ ) were significantly increased in the larger tumor group. Correlation analysis showed that tumor size was significantly correlated with the above elastic parameters ( $P < 0.05$ ). For inflammation, CRP was significantly increased in the larger tumor group ( $P < 0.001$ ) and positively correlated with tumor size ( $r = 0.249$ ,  $P = 0.0002$ ); neutrophils were also correlated with SWV peri-avg ( $r = 0.158$ ,  $P = 0.019$ ) ( $P < 0.05$ ). Conclusions: Tumor size in IDC patients is not only related to their ultrasonographic features but also reflects their inflammatory status.

**Keywords:** Invasive ductal carcinoma, tumor size, contrast-enhanced ultrasound, shear wave velocity, inflammation

## Introduction

Breast cancer is one of the most frequently diagnosed cancers in women around the world [1]. Reports indicate that in 2022, there were over 350,000 new cases of breast cancer among women in China, with approximately 75,000 deaths, accounting for approximately 15.6% and 8% of all new cancer cases and deaths, respectively [2]. Among these, invasive ductal carcinoma (IDC) is the most common histologic type, accounting for more than 80% of all breast cancer, with high heterogeneity and invasiveness [3, 4]. Tumor size plays a central role in the TNM staging system and has a direct effect on treatment planning and patient outcome [5]. The increase in tumor volume is often accompanied by a higher histologic

grade, a more active cell proliferation state, and a higher risk of lymph node metastasis. Therefore, the size of the mass is not only a morphologic feature but also an important indicator reflecting the biological behavior of breast cancer [6].

In recent years, with the development of ultrasound diagnostic technology, imaging approaches for evaluating breast tumors have become increasingly diverse [7]. Conventional ultrasound (CUS), as an important tool for routine screening and diagnosis of breast diseases, can provide basic information such as the shape, margin, echo type, calcification, and posterior echo attenuation of the mass to some extent [8]. On this basis, color Doppler can further assess the distribution of blood flow sig-

nals within and around the lesion. Virtual touch tissue imaging quantification (VTIQ), as a newly developed ultrasound elastography technique, can noninvasively measure the shear wave velocity (SWV) of tumor tissue, reflect its stiffness, and provide supplementary information for distinguishing between benign and malignant tumors [9]. In addition, contrast-enhanced ultrasound (CEUS) technology has been shown to be valuable for the diagnosis and grading of breast cancer by observing tumor microvascular perfusion characteristics in real time, which provides unique advantages for assessing tumor blood supply, infiltration boundaries, and enhancement patterns [10]. Although some studies have investigated the relationship between ultrasound features and the biological characteristics of breast cancer, recent research has indicated that the diagnostic success rate of ultrasound may vary for tumors of different sizes [11, 12]. Therefore, further comprehensive studies on the systematic correlation between ultrasound characteristics and mass size are still needed.

The role of inflammation in tumorigenesis and development has been increasingly emphasized, and systemic inflammatory response is not only involved in the regulation of the immune microenvironment of tumors, but also closely related to tumor aggressiveness, metastatic tendency and therapeutic response [13]. Inflammatory indicators such as neutrophils and C-reactive protein (CRP), as simple and easily accessible hematologic data, have prognostic value in various solid tumors [14-16]. However, in IDC, whether there is an intrinsic correlation among tumor size, ultrasound features, and inflammatory indicators remains unclear.

Based on this, this study intended to analyze retrospectively the multimodal ultrasound features (including CUS, CEUS, and VTIQ) and serum inflammatory indexes of IDC patients to investigate the correlation between them and the size of the mass. To our knowledge, few studies have simultaneously integrated multimodal ultrasound parameters with systemic inflammatory markers to explore their combined association with tumor size in IDC. This approach may reveal novel imaging-inflammation correlations that may enhance preoperative risk stratification and tailored treatment planning.

### Patients and methods

#### Case selection

This was a single-center retrospective study that included 218 female patients who attended The Affiliated Hospital of Bei-hua University from May 2022 to March 2025 and were diagnosed with IDC by pathology. Inclusion criteria: Baseline information is available and complete; Diagnosed with IDC; The CUS, VTIQ and CEUS examinations were completed before the operation; Complete CRP and neutrophil test results. Exclusion criteria: No clear pathologic diagnosis; Other types of breast cancer; Presence of serious infection; Presence of immune system disease or blood system disease; Baseline or test results incomplete. The diagnostic criteria for IDC in this study were based on the Guidelines for Breast Cancer Diagnosis and Treatment issued by the China Anti-Cancer Association, which provide standardized recommendations for imaging assessment, pathologic evaluation, and immunohistochemical testing to ensure accurate diagnosis [17]. This study was approved by the Ethics Committee of The Affiliated Hospital of Bei-hua University. Since this was a retrospective study, the requirement for informed consent from patients and their families was waived by the ethics committee.

#### Outcomes measures

All patients underwent preoperative color Doppler ultrasound using the Siemens ACUSON S3000 system, which was equipped with the VTIQ elastography module and CEUS analysis software. A 9L4 linear array probe was used, with a frequency of 4-9 MHz and a mechanical index of 0.08. Patients were examined in the supine or lateral position to fully expose both breasts and axillary regions.

First, the CUS examination was performed to record the location, aspect ratio, morphology, boundary, internal echo, calcification manifestation and posterior acoustic shadow and other characteristics of the lesion. Subsequently, color Doppler flow imaging was combined to assess the intensity of blood flow signals in the lesion and surrounding areas, and the blood flow grade classification was performed with reference to the Adler grading method (grade 0-III).

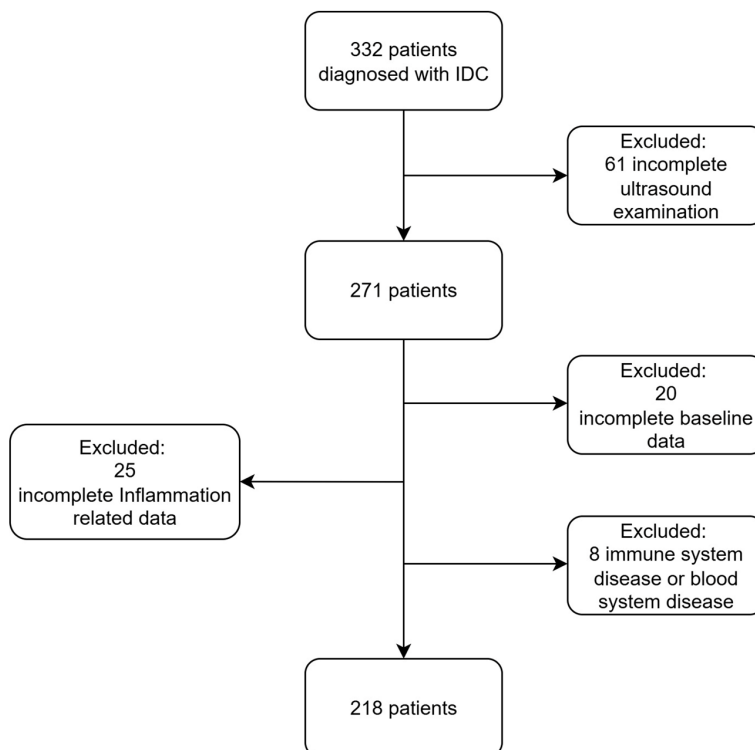


**Figure 1.** Flow chart for screening invasive ductal carcinoma (IDC) cases.

After completing CUS, we selected the largest section of the mass or the area with rich blood supply to initiate the CEUS mode. 2.4 mL of SonoVue contrast agent through the elbow vein were rapidly injected followed by immediately injecting 5 mL of normal saline for rinsing. The enhancement characteristics of the lesion were recorded in real time after angiography, such as the enhancement mode (fast advance and fast retreat/slow advance and slow retreat), the enhancement intensity (high/equal), whether the range expands after enhancement, and whether there is perfusion defect.

Elastography was performed using VTIQ mode. The probe was placed gently on the lesion, avoiding excessive pressure or interference from necrotic or liquefied areas. On a representative imaging plane, SWV values were measured, including the maximum (SWV max), minimum (SWV min), and the average SWV of peritumoral tissues (SWV peri-avg). Additionally, the SWV ratio between the lesion and surrounding glandular tissue (SWVR lesion/gland), as well as the SWVR max/min, were calculated.

Neutrophil counts were derived from peripheral venous blood samples analyzed by an automated hematology analyzer (BC-760 CS, Mindray). Serum CRP concentration was quantified using a clinical chemistry analyzer (BS-1000M, Mindray).

#### Data collection

Data collection included basic clinical information such as the patient's age, educational level, underlying diseases, tumor size, tumor side and location. Data of neutrophils and CRP in the blood routine were extracted. Patients were divided into two groups of  $> 2$  cm and  $\leq 2$  cm based on the maximum diameter of the mass in the pathology report [18, 19]. Neutrophil and CRP data were obtained from test results taken after the patient's admission but before surgery.

#### Primary and secondary outcomes

The primary outcomes were differences in ultrasound indicators among patients with different tumor sizes, the correlation between ultrasound indicators and tumor size, differences in inflammatory indicators among patients with different tumor sizes, and the correlation between inflammatory indicators and tumor size. The tumor size prediction model was a secondary outcome.

#### Statistical analysis

All data were statistically analyzed using SPSS 26.0 software. Measured data that conformed to a normal distribution were expressed as mean  $\pm$  standard deviation, and the independent sample t-test was used for comparison between groups. Data that were not normally distributed were expressed as median and interquartile range, and the Mann-Whitney U test was used for comparison between groups. Categorical variables were expressed as fre-

**Table 1.** Comparison of baseline characteristics between  $\leq 2$  cm and  $> 2$  cm tumor size groups

	$\leq 2$ cm Group (n = 78)	$> 2$ cm Group (n = 140)	Test statistic	P
Age	54.59 $\pm$ 9.96	55.03 $\pm$ 9.21	-0.33	0.744
BMI	20.67 $\pm$ 2.88	20.06 $\pm$ 3.02	1.46	0.147
Smoking			2.50	0.114
No	50 (64.10)	104 (74.29)		
Yes	28 (35.90)	36 (25.71)		
Alcohol Consumption			2.93	0.087
No	69 (88.46)	111 (79.29)		
Yes	9 (11.54)	29 (20.71)		
Menopause			2.69	0.101
No	18 (23.08)	20 (14.29)		
Yes	60 (76.92)	120 (85.71)		
Education Level			1.68	0.642
Primary school or below	45 (57.69)	76 (54.29)		
Junior high school	20 (25.64)	31 (22.14)		
Senior high school	11 (14.10)	26 (18.57)		
College or above	2 (2.56)	7 (5.00)		
Diabetes			0.28	0.597
No	54 (69.23)	92 (65.71)		
Yes	24 (30.77)	48 (34.29)		
Hypertension			1.20	0.273
No	18 (23.08)	42 (30.00)		
Yes	60 (76.92)	98 (70.00)		
Dyslipidemia			0.81	0.367
No	50 (64.10)	81 (57.86)		
Yes	28 (35.90)	59 (42.14)		
Coronary Heart Disease			0.96	0.326
No	61 (78.21)	117 (83.57)		
Yes	17 (21.79)	23 (16.43)		
History of Stroke			0.65	0.420
No	63 (80.77)	119 (85.00)		
Yes	15 (19.23)	21 (15.00)		

quencies and percentages and compared using the  $\chi^2$  test or Fisher's exact test, as appropriate. In addition, Spearman correlation analysis was conducted to explore the relationships between selected continuous variables, tumor size, and inflammatory markers. To examine further the factors related to tumor size, univariable logistic regression was performed for all demographic, ultrasound, and inflammatory variables. Variables with  $P < 0.10$  were subsequently included in a multivariable logistic regression to identify independent predictors, with odds ratios (ORs) and 95% confidence intervals (CIs) reported. For clarity of results, we ultimately presented only variables with  $P$ -values  $< 0.05$  in the multivariate logistic regression. A two-sided  $P$ -value  $< 0.05$  was

considered significant. We selected SWVR max/min as a representative predictor with a moderate effect size, and a post hoc power analysis (G\*Power 3.1.9.7), based on its adjusted OR of 1.75, event probability of 0.2,  $\alpha = 0.05$ , and total sample size of 218, indicated a statistical power of 94.6%, suggesting that the sample size was adequate to support the robustness of our findings.

## Results

### Comparison of baseline characteristics between tumor size groups

After screening, as shown in **Figure 1**, data from a total of 218 IDC patients were included

## Ultrasonographic characteristics of breast invasive ductal carcinoma

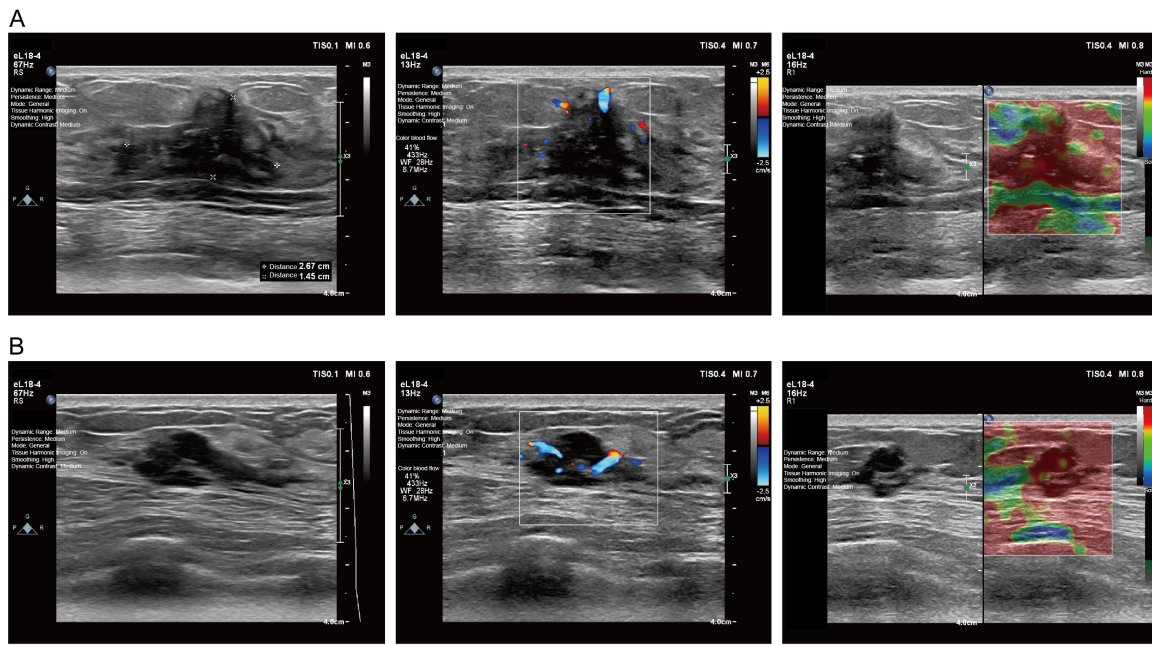


**Figure 2.** Representative ultrasound pictures of the patients. A. Patient 1, female, 61 years old, had a mass located in the upper outer quadrant of the left breast, measuring  $2.6 \times 1.4 \times 1.9$  cm, with pathologic findings of invasive ductal carcinoma. From left to right are shown conventional ultrasound (CUS), color Doppler flow imaging, and virtual touch tissue imaging quantification (VTIQ). CUS demonstrates an irregularly marginated mass; color Doppler reveals abundant blood flow signals within and around the lesion; VTIQ indicates that most of the lesion area is displayed as warm colors, suggesting relatively high stiffness, with the range of hardness slightly exceeding the grayscale boundary. B. Patient 2, female, 58 years old, had a mass located in the upper inner quadrant of the left breast measuring  $2.4 \times 1.8 \times 1.4$  cm, with pathologic findings of invasive ductal carcinoma. From left to right are shown CUS, color Doppler flow imaging, and VTIQ. CUS demonstrates a relatively small mass with clear margins; color Doppler shows a few punctate and short strip-shaped blood flow signals within the lesion; VTIQ reveals warm colors in the central or partial areas of the lesion, while the periphery is predominantly yellow-green, and the range of hardness is largely confined within the grayscale boundary.

**Table 2.** Comparison of conventional ultrasound features between tumor size groups

	$\leq 2$ cm Group (n = 78)	$> 2$ cm Group (n = 140)	Test statistic	P
Tumor location			10.37	0.035
Upper Inner Quadrant	18 (23.08)	15 (10.71)		
Lower Inner Quadrant	9 (11.54)	15 (10.71)		
Upper Outer Quadrant	32 (41.03)	85 (60.71)		
Lower Outer Quadrant	10 (12.82)	16 (11.43)		
Periareolar Area	9 (11.54)	9 (6.43)		
Aspect ratio			2.48	0.115
$\leq 1$	68 (87.18)	110 (78.57)		
$> 1$	10 (12.82)	30 (21.43)		
Posterior acoustic attenuation			0.08	0.773
No attenuation	26 (33.33)	44 (31.43)		
Attenuation or Disappearance	52 (66.67)	96 (68.57)		
Spiculated margin			0.92	0.337
No	41 (52.56)	83 (59.29)		
Yes	37 (47.44)	57 (40.71)		
Adler blood flow grading			8.75	0.003
Grade 0-I	36 (46.15)	37 (26.43)		
Grade II-III	42 (53.85)	103 (73.57)		

## Ultrasonographic characteristics of breast invasive ductal carcinoma

**Table 3.** Comparison of contrast-enhanced ultrasound features between tumor size groups

	≤ 2 cm Group (n = 78)	> 2 cm Group (n = 140)	Test statistic	P
Enhancement intensity			5.71	0.017
High enhancement	61 (78.21)	126 (90.00)		
Iso- or low enhancement	17 (21.79)	14 (10.00)		
Enhancement speed			2.58	0.108
Rapid	25 (32.05)	31 (22.14)		
Slow or absent	53 (67.95)	109 (77.86)		
Enhancement pattern			2.54	0.281
Centripetal	53 (67.95)	98 (70.00)		
Centrifugal	10 (12.82)	25 (17.86)		
Diffuse	15 (19.23)	17 (12.14)		
Perfusion defect			0.80	0.371
Absent	28 (35.90)	42 (30.00)		
Present	50 (64.10)	98 (70.00)		
Post-enhancement size change			4.51	0.034
Enlargement	55 (70.51)	116 (82.86)		
No change or reduction	23 (29.49)	24 (17.14)		

**Table 4.** Comparison of virtual touch tissue imaging quantification (VTIQ) parameters between tumor size groups

	≤ 2 cm Group (n = 78)	> 2 cm Group (n = 140)	Test statistic	P
Shear wave velocity (SWV) <sub>max</sub>	6.00 (5.00, 6.80)	6.40 (5.07, 7.93)	-2.13	0.033
SWV <sub>min</sub>	2.70 (2.40, 3.00)	2.50 (2.20, 2.90)	-1.60	0.110
SWV <sub>peri-avg</sub>	4.40 (3.82, 4.88)	4.70 (4.00, 5.20)	-2.57	0.010
SWVR <sub>max/min</sub>	2.29 (1.88, 2.58)	2.47 (1.96, 3.24)	-2.62	0.009
SWVR <sub>lesion/gland</sub>	1.37 (1.11, 1.72)	1.38 (1.08, 1.82)	-0.24	0.811

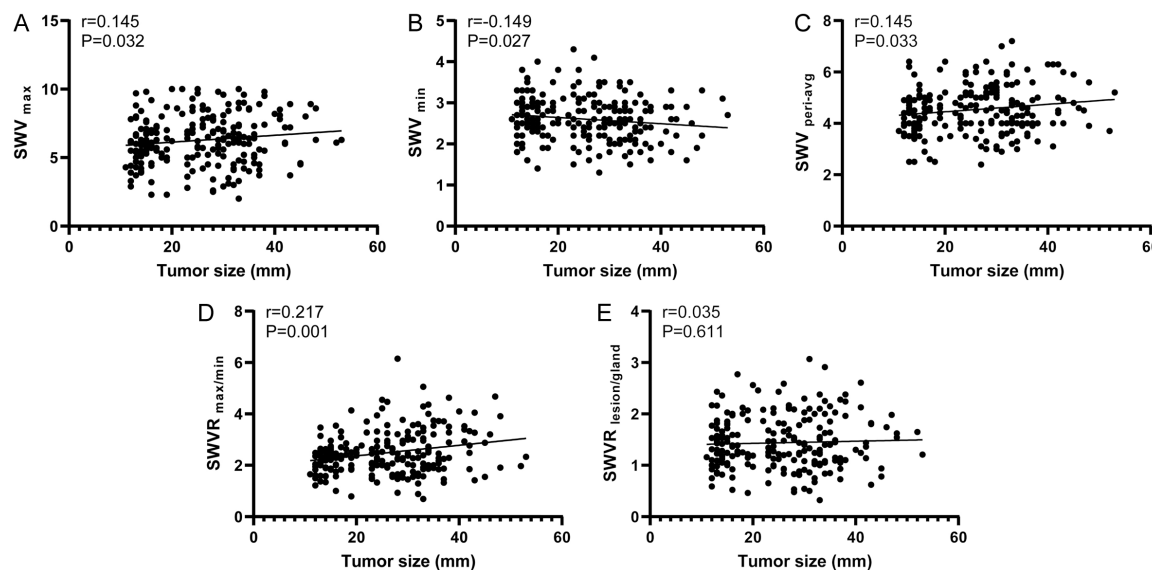


**Figure 3.** Correlation analysis between tumor size and virtual touch tissue imaging quantification (VTIQ) features. A. Scatter plot showing correlation between tumor size and shear wave velocity (SWV) max. B. Scatter plot showing correlation between tumor size and SWV min. C. Scatter plot showing correlation between tumor size and SWV peri-avg. D. Scatter plot showing correlation between tumor size and SWVR max/min. E. Scatter plot showing correlation between tumor size and SWVR lesion/gland.

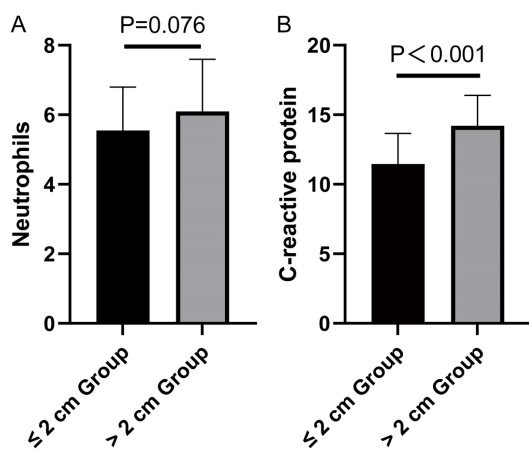


**Figure 4.** Comparison of neutrophil count and C-reactive protein (CRP) levels between tumor size groups. A. Results of neutrophil count. B. Results of CRP.

in the analysis. According to the maximum tumor diameter, the enrolled IDC patients were divided into two groups:  $\leq 2$  cm ( $n = 78$ ) and  $> 2$  cm ( $n = 140$ ). As shown in **Table 1**, there were no significant differences between the two groups in terms of age, BMI, or education level ( $P > 0.05$ ). As important lifestyle factors, the proportions of smokers and alcohol consumers were slightly higher in the  $> 2$  cm group, but the differences were not significant ( $P > 0.05$ ). Likewise, the proportion of postmenopausal patients did not differ significantly between the two groups ( $P > 0.05$ ). In addition, common geriatric comorbidities including diabetes mellitus, hypertension, dyslipidemia, coronary artery disease, and history of stroke were also distributed close to each other between the two groups (all,  $P > 0.05$ ). In summary, the results of this section indicate that the two groups of patients have similar baseline characteristics, and were comparable for subsequent analysis.

#### Comparison of conventional ultrasound features between tumor size groups

The ultrasound representative pictures of the patients are shown in **Figure 2**. As shown in **Table 2**, the features of CUS showed some differences in the spatial distribution of tumors between the two groups of patients, with lesions in the  $> 2$  cm group more often located in the outer upper quadrant, whereas the tumor locations of the patients in the  $\leq 2$  cm group were more dispersed, and this difference was

statistically significant ( $P = 0.035$ ). In terms of blood flow signals, Adler grading showed that the proportion of grade II-III blood flow in the  $> 2$  cm group was significantly higher than that in the  $\leq 2$  cm group ( $P = 0.003$ ), suggesting that larger tumors may be associated with richer blood perfusion. However, for other features such as aspect ratio, posterior acoustic attenuation, and spiculated margins, the distributions between the two groups were similar ( $P > 0.05$ ).

#### Comparison of contrast-enhanced ultrasound features between tumor size groups

As shown in **Table 3**, differences were observed between the two groups in terms of CEUS parameters. Specifically, the proportion of lesions showing high enhancement was significantly higher in the  $> 2$  cm group compared to the  $\leq 2$  cm group ( $P = 0.017$ ). Although the rate of enhancement and the pattern of enhancement (centripetal, centrifugal, or diffuse) were distributed slightly differently between the two groups, the statistical differences were not significant, nor were there any significant differences in the characteristics of the perfusion defects (all,  $P > 0.05$ ). Notably, the proportion of individuals with post-enhancement range expansion was significantly higher in the  $> 2$  cm group than in the  $\leq 2$  cm group ( $P = 0.034$ ). This suggests that larger lesions exhibit more extensive contrast expansion with CEUS.

#### Distribution of VTIQ parameters in different tumor size groups and correlation with tumor size

As shown in **Table 4**, in terms of VTIQ parameters, SWV max values were significantly higher in the  $> 2$  cm group than in the  $\leq 2$  cm group ( $P = 0.033$ ), suggesting that the internal tissues of larger lesions may be more rigid. SWV per\_avg and SWVR max/min were also significantly higher in the  $> 2$  cm group ( $P = 0.010$ ,  $P = 0.009$ ), indicating that the periphery of the larger lesions and the internal SWV changes were greater. Notably, there was no significant difference between the SWVR lesion/gland and SWVR min in either group ( $P > 0.05$ ). Furthermore, as shown in **Figure 3**, Spearman's correlation analysis revealed no significant correlation between SWVR lesion/gland and tumor size ( $P > 0.05$ ). In contrast, maximum tumor diameter was positively correlated with SWV

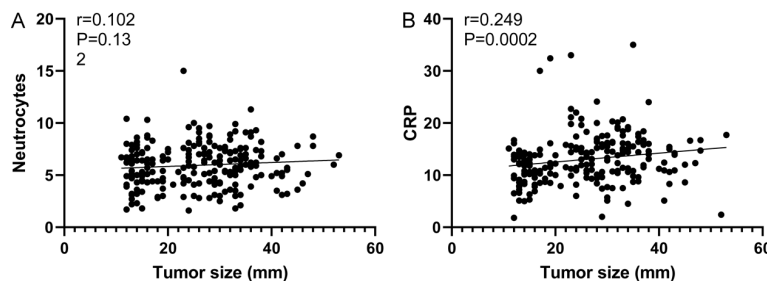


**Figure 5.** Correlation analysis between tumor size and systemic inflammatory markers. A. Scatter plot showing correlation between tumor size and neutrophil count. B. Scatter plot showing correlation between tumor size and CRP levels.

max ( $r = 0.145$ ,  $P = 0.032$ ), SWV peri-avg ( $r = 0.145$ ,  $P = 0.033$ ), and SWVR max/min ( $r = 0.217$ ,  $P = 0.001$ ), and negatively correlated with SWV min ( $r = -0.149$ ,  $P = 0.027$ ).

#### Relationship between tumor size and inflammatory markers

We also analyzed systemic inflammatory markers between the two groups. As shown in **Figure 4**, both neutrophil count and CRP levels were higher in the  $> 2$  cm group compared to the  $\leq 2$  cm group. The difference in CRP levels was significant ( $P < 0.001$ ), while the difference in neutrophil count approached significance ( $P = 0.076$ ). In addition, as shown in **Figure 5**, Spearman's correlation analysis revealed that the maximum tumor diameter showed a positive correlation with CRP ( $r = 0.249$ ,  $P = 0.0002$ ), whereas the correlation with neutrophil count was not significant ( $r = 0.102$ ,  $P = 0.132$ ).

#### Correlation between VTIQ parameters and inflammatory markers

We further analyzed the correlations between ultrasound parameters and inflammatory markers. As shown in **Figure 6**, among the VTIQ parameters, only SWV peri-avg showed a significant positive correlation with neutrophil count ( $r = 0.158$ ,  $P = 0.019$ ). Other parameters, including SWV max and SWVR max/min, were not significantly correlated with either neutrophil count or CRP levels ( $P > 0.05$ ). The results suggest that the elastic characteristics of breast cancer tumors may be affected by local inflammatory responses to some extent.

#### Univariable and multivariable logistic regression analysis of factors associated with tumor size

The variable assignment in the regression analysis is shown in **Table 5**. As shown in **Table 6**, the univariable logistic regression analysis, alcohol consumption, tumor location, Adler blood flow grading, enhancement intensity, post-enhancement size change, SWV max, SWV peri-avg, SWVR max/min, and inflammatory markers such as neutrophils and CRP were associated with tumor size ( $P < 0.1$ ). As shown in **Table 7**, in the multivariable logistic regression analysis, alcohol consumption ( $P = 0.034$ , OR = 2.94), tumor location (Upper Outer Quadrant,  $P = 0.003$ , OR = 4.40), Adler blood flow grading (Grade II-III,  $P = 0.005$ , OR = 2.73), enhancement intensity (Iso- or low-enhancement,  $P = 0.008$ , OR = 0.29), post-enhancement size change (No change or reduction,  $P = 0.027$ , OR = 0.40), as well as SWV peri-avg ( $P = 0.006$ , OR = 1.75), SWVR max/min ( $P = 0.009$ , OR = 2.79), Neutrophils ( $P = 0.03$ , OR = 1.22), and CRP ( $P = 0.005$ , OR = 1.12) remained significant.

#### Discussion

This study examined the relationship between ultrasound features, tumor size, and inflammatory indicators in IDC patients. We assessed multimodal imaging parameters in breast cancer using CUS, CEUS, and VTIQ and combined them with hematologic inflammatory indicators. We found that the larger tumor group exhibited significant differences in several ultrasound parameters compared to the smaller tumor group. Some of these parameters were statistically correlated with the maximum tumor diameter. Meanwhile, there was a positive correlation between tumor size and CRP, and some VTIQ parameters showed a degree of correlation with inflammatory indexes. Furthermore, logistic regression analysis identified several independent predictors of larger tumor size, including tumor location, Adler blood flow grading, enhancement intensity, post-enhancement size change, SWV peri-avg, SWVR max/min, neutrophils, and CRP. These

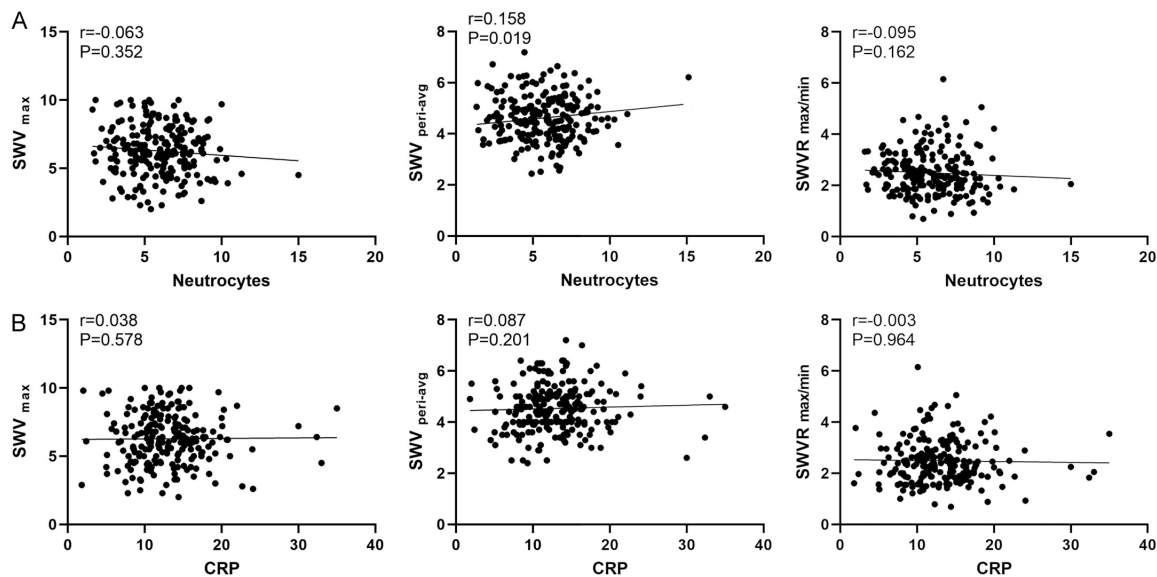


**Figure 6.** Correlation between VTIQ parameters and inflammatory markers. A. Scatter plot showing correlation between VTIQ parameters and Neutrocytes. B. Scatter plot showing correlation between VTIQ parameters and CRP.

results suggest that tumor size was closely related not only to morphological characteristics but also to internal biological behavior and immune-inflammatory response.

As an important tool for breast cancer screening and initial diagnosis, CUS is valuable for assessing tumor morphology and classification [20]. In the present study, we found that larger tumors were more commonly found in the upper outer quadrant of the breast, which is consistent with previous reports, and the reason for this may be related to the more complex structure of the mammary glands in this region [21, 22]. However, it is worth noting that an earlier study by Lee et al. that included breast cancer patients showed a greater volume of tumors in the central quadrant, which warrants further investigation [23]. Regarding blood flow distribution, prior studies have shown that in both renal cell carcinoma and breast cancer, larger tumors tend to present with higher Adler grades, this finding is understandable, as although larger tumors do not necessarily have stronger angiogenic capability, they generally possess richer blood supply [21, 24, 25]. In the present study, we found that patients with IDC whose tumor size was greater than 2 cm had significantly higher Adler grading than patients with smaller tumors, which is consistent with the aforementioned studies. It is noteworthy that parameters such as aspect ratio, spiculat-

ed margins, and posterior acoustic attenuation did not differ significantly between the two groups in our study. This may be because all enrolled patients had IDC, leading to a relative homogeneity of tumor type.

CEUS is capable of dynamically observing the microvascular perfusion and blood flow distribution of a lesion, providing visual imaging of the tumor's microenvironment [10, 20]. A previous study involving breast cancer patients reported that the enhancement intensity and range on ultrasound were significantly higher in patients with larger tumors compared to those with smaller tumors [26]. Meanwhile, a study analyzing 1059 patients found that tumor size was strongly correlated with the enhancement characteristics of CEUS, which was mainly demonstrated by the fact that larger tumors showed higher enhancement intensity and wider enhancement range in CEUS [27]. In line with these findings, our study also demonstrated that patients in the larger tumor group had significantly higher rates of hyper-enhancement and post-enhancement range expansion compared to the small tumor group. In addition, the increase in tumor size may lead to uneven distribution of the vascular system and internal necrosis, which may affect the enhancement pattern of CEUS [27]. In our study, no significant differences were observed between the two groups in terms of enhancement patterns

## Ultrasonographic characteristics of breast invasive ductal carcinoma

**Table 5.** Variable assignment

Variable	Coding Scheme	Type	Reference
Tumor Size	0 = $\leq$ 2 cm; 1 = $>$ 2 cm	Categorical variable	0
Age	Original value (years)	Continuous variable	-
BMI	Original value ( $\text{kg}/\text{m}^2$ )	Continuous variable	-
Smoking	0 = No; 1 = Yes	Categorical variable	0
Alcohol Consumption	0 = No; 1 = Yes	Categorical variable	0
Menopause	0 = No; 1 = Yes	Categorical variable	0
Education Level	1 = Primary school or below; 2 = Junior high school; 3 = Senior high school; 4 = College or above	Categorical variable	1
Diabetes	0 = No; 1 = Yes	Categorical variable	0
Hypertension	0 = No; 1 = Yes	Categorical variable	0
Dyslipidemia	0 = No; 1 = Yes	Categorical variable	0
Coronary Heart Disease	0 = No; 1 = Yes	Categorical variable	0
History of Stroke	0 = No; 1 = Yes	Categorical variable	0
Tumor Location	1 = Upper Inner Quadrant; 2 = Lower Inner Quadrant; 3 = Upper Outer Quadrant; 4 = Lower Outer Quadrant; 5 = Periareolar Area	Categorical variable	1
Aspect Ratio	0 = $\leq$ 1; 1 = $>$ 1	Categorical variable	0
Posterior Acoustic Attenuation	0 = No attenuation; 1 = Attenuation or Disappearance	Categorical variable	0
Spiculated Margin	0 = No; 1 = Yes	Categorical variable	0
Adler Blood Flow Grading	0 = Grade 0-I; 1 = Grade II-III	Categorical variable	0
Enhancement Intensity	0 = High enhancement; 1 = Iso- or low enhancement	Categorical variable	0
Enhancement Speed	0 = Rapid; 1 = Slow or absent	Categorical variable	0
Enhancement Pattern	0 = Centripetal; 1 = Centrifugal; 2 = Diffuse	Categorical variable	0
Perfusion Defect	0 = Absent; 1 = Present	Categorical variable	0
Post-enhancement Size Change	0 = Enlargement; 1 = No change or reduction	Categorical variable	0
SWV max	Original value ( $\text{m}/\text{s}$ )	Continuous variable	-
SWV min	Original value ( $\text{m}/\text{s}$ )	Continuous variable	-
SWV peri-avg	Original value ( $\text{m}/\text{s}$ )	Continuous variable	-
SWVR max/min	Original value	Continuous variable	-
SWVR lesion/gland	Original value	Continuous variable	-
Neutrophils	Original value ( $\times 10^9/\text{L}$ )	Continuous variable	-
CRP	Original value ( $\text{mg}/\text{L}$ )	Continuous variable	-

or perfusion defects. This suggests that these parameters may be influenced more by the homogeneity of the tumor's internal vascular architecture than by tumor size alone. Overall, CEUS has unique advantages in evaluating tumor infiltration margins; however, the sensitivity of certain CEUS parameters to tumor size requires validation in larger studies.

Elastography, as a new ultrasound technique that has developed rapidly in recent years, has shown good prospects in noninvasively assessing tissue stiffness and reflecting the degree of

tumor malignancy. Among its methods, VTIQ enables objective and quantitative evaluation of tissue elasticity by measuring SWV, providing important imaging evidence for distinguishing between benign and malignant tumors [28]. Previous studies have shown that SWV is significantly positively correlated with tumor size and is also higher in triple-negative breast cancers and tumors with strong invasion [29]. In our study, we found that VTIQ parameters were significantly elevated in the larger tumor group, and all were positively correlated with tumor diameter, suggesting that larger tumors tend to

## Ultrasonographic characteristics of breast invasive ductal carcinoma

**Table 6.** Univariable logistic regression analysis of factors associated with tumor size

Variable	$\beta$	S.E.	P	OR (95% CI)
Age	0.00	0.01	0.742	1.00 (0.98-1.03)
BMI	-0.07	0.05	0.148	0.93 (0.85-1.03)
Smoking				
No				1.00
Yes	-0.48	0.31	0.115	0.62 (0.34-1.12)
Alcohol Consumption				
No				1.00
Yes	0.69	0.41	0.091	2.00 (0.89-4.48)
Menopause				
No				1.00
Yes	0.59		0.104	1.80 (0.89-3.65)
Education Level				
Primary school or below				1.00
Junior high school	-0.09	0.34	0.802	0.92 (0.47-1.80)
Senior high school	0.34	0.41	0.408	1.40 (0.63-3.10)
College or above	0.73	0.82	0.376	2.07 (0.41-10.41)
Diabetes				
No				1.00
Yes	0.16	0.30	0.597	1.17 (0.65-2.13)
Hypertension				
No				1.00
Yes	-0.36	0.33	0.274	0.70 (0.37-1.33)
Dyslipidemia				
No				1.00
Yes	0.26	0.29	0.367	1.30 (0.73-2.30)
Coronary Heart Disease,				
No				1.00
Yes	-0.35	0.36	0.328	0.71 (0.35-1.42)
History of Stroke				
No				1.00
Yes	-0.30	0.37	0.421	0.74 (0.36-1.54)
Tumor location				
Upper Inner Quadrant				1.00
Lower Inner Quadrant	0.69	0.55	0.206	2.00 (0.68-5.85)
Upper Outer Quadrant	1.16	0.41	0.004	3.19 (1.44-7.07)
Lower Outer Quadrant	0.65	0.53	0.222	1.92 (0.67-5.46)
Periareolar Area	0.18	0.59	0.756	1.20 (0.38-3.79)
Aspect ratio				
≤ 1				1.00
> 1	0.62	0.40	0.119	1.85 (0.85-4.03)
Posterior acoustic attenuation				
No attenuation				1.00
Attenuation or Disappearance	0.09	0.30	0.773	1.09 (0.60-1.97)
Spiculated margin				
No				1.00
Yes	-0.27	0.28	0.337	0.76 (0.44-1.33)

## Ultrasonographic characteristics of breast invasive ductal carcinoma

Adler blood flow grading				
Grade 0-I				1.00
Grade II-III	0.87	0.30	0.003	2.39 (1.33-4.27)
Enhancement intensity				
High enhancement				1.00
Iso- or low enhancement	-0.92	0.39	0.019	0.40 (0.18-0.86)
Enhancement speed				
Rapid				1.00
Slow or absent	0.51	0.32	0.110	1.66 (0.89-3.09)
Enhancement pattern				
Centripetal				1.00
Centrifugal	0.30	0.41	0.463	1.35 (0.60-3.03)
Diffuse	-0.49	0.39	0.213	0.61 (0.28-1.32)
Perfusion defect				
Absent				1.00
Present	0.27	0.30	0.372	1.31 (0.73-2.35)
Post-enhancement size change				
Enlargement				1.00
No change or reduction	-0.70	0.33	0.035	0.49 (0.26-0.95)
$SWV_{max}$	0.15	0.08	0.051	1.17 (1.00-1.36)
$SWV_{min}$	-0.41	0.27	0.131	0.66 (0.39-1.13)
$SWV_{peri-avg}$	0.42	0.17	0.013	1.52 (1.09-2.10)
$SWVR_{max/min}$	0.60	0.20	0.002	1.82 (1.24-2.67)
$SWVR_{lesion/gland}$	0.11	0.28	0.690	1.12 (0.65-1.93)
Neutrophils	0.13	0.07	0.062	1.14 (0.99-1.32)
CRP	0.13	0.04	< 0.001	1.14 (1.06-1.22)

OR: odds ratio, CI: confidence interval.

exhibit increased stiffness both within and around the lesion. Notably, we found that SWV<sub>min</sub> was negatively correlated with tumor size, a result that is relatively rare in the existing literature. We speculate that this phenomenon may be due to necrosis, liquefied areas, or non-solid tissue components commonly found in larger tumors, which result in lower SWV readings on certain ultrasound views [30]. However, this proposed mechanism requires further validation, and caution should be exercised when interpreting these results. Additionally, there was no significant difference in SWVR<sub>lesion/gland</sub> between groups, and it was not correlated with tumor size. This suggests that the heterogeneity of breast tissue structure may also influence this parameter.

Inflammatory responses are key factors in tumor initiation and progression. In breast cancer in particular, systemic inflammatory status has been shown to be closely associated with disease prognosis [31, 32]. In this study, CRP

was found to be significantly elevated in the larger tumor group and positively correlated with tumor diameter, which is closely related to the fact that CRP reflects tissue damage and tumor-associated inflammatory state. Similar to our results, a previous study demonstrated that pro-inflammatory cytokines such as interleukin-6 were significantly associated with tumor size and disease stage in type I endometrial carcinoma [33]. Further analysis revealed a positive correlation between SWV<sub>peri-avg</sub> and neutrophil count, suggesting a potential link between local tissue stiffness and the degree of inflammatory cell infiltration. This finding is in line with the biological mechanism whereby immune cells within the tumor microenvironment promote extracellular matrix remodeling and tissue stiffening through the release of cytokines [34]. However, no significant association was observed between the remaining VTIQ parameters and inflammation indicators. This suggests that, although ultrasound elastography can reflect tissue state, its

## Ultrasonographic characteristics of breast invasive ductal carcinoma

**Table 7.** Multivariable logistic regression analysis of factors associated with tumor size

Variable	$\beta$	S.E.	P	OR (95% CI)
Alcohol Consumption				
No				1.00
Yes	1.08	0.51	0.034	2.94 (1.09-7.96)
Tumor location				
Upper Inner Quadrant				1.00
Lower Inner Quadrant	0.91	0.66	0.167	2.49 (0.68-9.05)
Upper Outer Quadrant	1.48	0.49	0.003	4.40 (1.68-11.52)
Lower Outer Quadrant	1.02	0.63	0.105	2.77 (0.81-9.48)
Periareolar Area	1.03	0.72	0.148	2.81 (0.69-11.43)
Adler blood flow grading				
Grade 0-I				1.00
Grade II-III	1.00	0.36	0.005	2.73 (1.35-5.55)
Enhancement intensity				
High enhancement				1.00
Iso- or low enhancement	-1.25	0.48	0.008	0.29 (0.11-0.73)
Post-enhancement size change				
Enlargement				1.00
No change or reduction	-0.91	0.41	0.027	0.40 (0.18-0.90)
$SWV_{peri-avg}$	0.56	0.21	0.006	1.75 (1.17-2.63)
$SWVR_{max/min}$	1.02	0.39	0.009	2.79 (1.29-6.01)
Neutrophils	0.20	0.09	0.030	1.22 (1.02-1.47)
CRP	0.12	0.04	0.005	1.12 (1.04-1.22)

OR: odds ratio, CI: confidence interval.

correlation with systemic inflammation state is unstable. Further study of joint detection of local cytokines may be warranted.

However, this study had certain limitations. First, as a single-center retrospective study, it was difficult to avoid potential selection bias. Second, the acquisition of ultrasound parameters was dependent on operator experience, and although it was done by a senior physician, it was still difficult to completely exclude subjective errors. Third, the CEUS features analyzed were primarily qualitative or semi-quantitative. As such, correlating these features with continuous variables like tumor size and inflammatory markers was not methodologically pursued. Fourth, this study did not include cross-validation of the imaging findings with biological markers such as Ki-67, which limits a deeper interpretation of the tumor's biological behavior. In addition to the above limitations, future studies could consider incorporating multicenter data and tracking tumor progression and treatment response to further explore

the causal relationships between various ultrasound features and the prognosis of IDC.

### Conclusion

This study preliminarily established the associations between tumor size, imaging features, and immune status from the perspectives of ultrasound imaging and inflammation, providing theoretical support for the diagnosis and treatment of IDC.

### Acknowledgements

This work was supported by Jilin Provincial Department of Education Project (JJKH2020-0064KJ).

### Disclosure of conflict of interest

None.

**Address correspondence to:** Xiao-Hong Liu, Department of Ultrasound, The Affiliated Hospital of Bei-Hua University, No. 12 Jiefang Middle Road,

Chuanying District, Jilin 132000, Jilin, China. Tel: +86-0432-62166228; E-mail: bhlxhn@126.com

## References

- [1] Giaquinto AN, Sung H, Newman LA, Freedman RA, Smith RA, Star J, Jemal A and Siegel RL. Breast cancer statistics 2024. *CA Cancer J Clin* 2024; 74: 477-495.
- [2] Sun K, Zhang B, Lei S, Zheng R, Liang X, Li L, Feng X, Zhang S, Zeng H, Yao Y, Ma P, Wang S, Chen R, Han B, Wei W and He J. Incidence, mortality, and disability-adjusted life years of female breast cancer in China, 2022. *Chin Med J (Engl)* 2024; 137: 2429-2436.
- [3] Raghavendra AS, Bassett R Jr, Damodaran S, Barcenas CH, Mouabbi JA, Layman R and Tripathy D. Clinical characteristics and survival outcomes of metastatic invasive lobular and ductal carcinoma. *JAMA Netw Open* 2025; 8: e251888.
- [4] Gallas AE, Morenikeji GO, King RE, Adegbaju MS, Ayoola A, Taiwo G and Morenikeji OB. An overview of Invasive Ductal Carcinoma (IDC) in women's breast cancer. *Curr Mol Med* 2025; 25: 361-371.
- [5] Zheng YZ, Wang L, Hu X and Shao ZM. Effect of tumor size on breast cancer-specific survival stratified by joint hormone receptor status in a SEER population-based study. *Oncotarget* 2015; 6: 22985-22995.
- [6] Liu Y, He M, Zuo WJ, Hao S, Wang ZH and Shao ZM. Tumor size still impacts prognosis in breast cancer with extensive nodal involvement. *Front Oncol* 2021; 11: 585613.
- [7] Li G, Huang X, Wu H, Tian H, Huang Z, Wang M, Liu Q, Xu J, Cui L and Dong F. Enhancing early breast cancer diagnosis with contrast-enhanced ultrasound radiomics: insights from intratumoral and peritumoral analysis. *Clin Breast Cancer* 2025; 25: 180-191.
- [8] Gokhale S. Ultrasound characterization of breast masses. *Indian J Radiol Imaging* 2009; 19: 242-247.
- [9] Lian W, Lian K and Lin T. Breast imaging reporting and data system evaluation of breast lesions improved with virtual touch tissue imaging average grayscale values. *Technol Health Care* 2024; 32: 925-936.
- [10] Li LL, Su QL, Deng YX, Guo WW, Lun HM and Hu Q. Contrast-enhanced ultrasound for the preoperative prediction of pathological characteristics in breast cancer. *Front Oncol* 2024; 14: 1320714.
- [11] Liu Y, Liao X, He Y, He F, Ren J, Zhou P and Zhang X. Tumor size and stage assessment accuracy of MRI and ultrasound versus pathological measurements in early breast cancer patients. *BMC Womens Health* 2025; 25: 159.
- [12] Stachs A, Pandjaitan A, Martin A, Stubert J, Hartmann S, Gerber B and Glass Å. Accuracy of tumor sizing in breast cancer: a comparison of strain elastography, 3-D ultrasound and conventional B-mode ultrasound with and without compound imaging. *Ultrasound Med Biol* 2016; 42: 2758-2765.
- [13] Nishida A and Andoh A. The role of inflammation in cancer: mechanisms of tumor initiation, progression, and metastasis. *Cells* 2025; 14: 488.
- [14] Alshamsan B, Elshenawy MA, Aseafan M, Fahmy N, Badran A, Elhassan T, Alsayed A, Suleiman K and Al-Tweigeri T. Prognostic significance of the neutrophil to lymphocyte ratio in locally advanced breast cancer. *Oncol Lett* 2024; 28: 429.
- [15] Qi X, Chen J, Wei S, Ni J, Song L, Jin C, Yang L and Zhang X. Prognostic significance of platelet-to-lymphocyte ratio (PLR) in patients with breast cancer treated with neoadjuvant chemotherapy: a meta-analysis. *BMJ Open* 2023; 13: e074874.
- [16] Kim ES, Kim SY and Moon A. C-reactive protein signaling pathways in tumor progression. *Biomol Ther* 2023; 31: 473-483.
- [17] The Society of Breast Cancer China Anti-Cancer Association and Breast Oncology Group of the Oncology Branch of the Chinese Medical Association. Guidelines for breast cancer diagnosis and treatment by China Anti-cancer Association (2024 edition). *Zhongguo Aizheng Zazhi* 2023; 33: 1092-1186.
- [18] van de Voort EMF, Struik GM, Birnie E, Moelker A, Verhoef C and Klem TMAL. Thermal ablation as an alternative for surgical resection of small ( $\leq 2$  cm) breast cancers: a meta-analysis. *Clin Breast Cancer* 2021; 21: e715-e730.
- [19] Strand F, Humphreys K, Holm J, Eriksson M, Törnberg S, Hall P, Azavedo E and Czene K. Long-term prognostic implications of risk factors associated with tumor size: a case study of women regularly attending screening. *Breast Cancer Res* 2018; 20: 31.
- [20] Li X, Zhang J, Zhang G, Liu J, Tang C, Chen K, Chen P, Tan L and Guo Y. Contrast-enhanced ultrasound and conventional ultrasound characteristics of breast cancer with different molecular subtypes. *Clin Breast Cancer* 2024; 24: 204-214.
- [21] Li W, Cao C, Shi L, Wang Z and Li J. Correlation analysis between tumor size and multimodal ultrasound and immune markers in breast invasive ductal carcinoma. *Radiol Pract* 2024; 39: 540-546.
- [22] Lee AH. Why is carcinoma of the breast more frequent in the upper outer quadrant? A case series based on needle core biopsy diagnoses. *Breast* 2005; 14: 151-152.

## Ultrasonographic characteristics of breast invasive ductal carcinoma

- [23] Rummel S, Hueman MT, Costantino N, Shriver CD and Ellsworth RE. Tumour location within the breast: does tumour site have prognostic ability? *Ecancermedicalscience* 2015; 9: 552.
- [24] Cheng J, Wang Y, Wei L, Cheng R, Jiang J, Cui X and Dong Y. The analysis of multimodality ultrasound features of renal cell carcinomas with different tumor sizes. *Clin Hemorheol Microcirc* 2025; 90: 51-59.
- [25] Sckell A, Safabakhsh N, Dellian M and Jain RK. Primary tumor size-dependent inhibition of angiogenesis at a secondary site: an intravital microscopic study in mice. *Cancer Res* 1998; 58: 5866-5869.
- [26] Leng X, Huang G and Ma F. The correlation between lesion size and contrast-enhanced ultrasound in breast cancer. *Zhonghua Chao Sheng Ying Xiang Xue Za Zhi* 2015; 24: 324-327.
- [27] Fu N, Li J, Wang B, Jiang Y, Li S, Niu R and Wang Z. Diagnostic performance of contrast-enhanced ultrasound in breast lesions: what diagnostic models could be used for lesions of different sizes? *Gland Surg* 2023; 12: 1654-1667.
- [28] Togawa R, Riedel F, Feisst M, Fastner S, Gomez C, Hennigs A, Nees J, Pfob A, Schäfgen B, Stieber A, Wallwiener M, Heil J and Golatta M. Shear-wave elastography as a supplementary tool for axillary staging in patients undergoing breast cancer diagnosis. *Insights Imaging* 2024; 15: 196.
- [29] Kwon M, Youn I, Ko ES and Choi SH. Correlation of shear-wave elastography stiffness and apparent diffusion coefficient values with tumor characteristics in breast cancer. *Sci Rep* 2024; 14: 7180.
- [30] Vitale I, Shema E, Loi S and Galluzzi L. Intratumoral heterogeneity in cancer progression and response to immunotherapy. *Nat Med* 2021; 27: 212-224.
- [31] Bakker NAM, Garner H, van Dyk E, Champanhet E, Klaver C, Duijst M, Voorwerk L, Nederlof I, Voorthuis R, Liefaard MC, Nieuwland M, de Rink I, Bleijerveld OB, Oosterkamp HM, Wessels LFA, Kok M and de Visser KE. Triple-negative breast cancer modifies the systemic immune landscape and alters neutrophil functionality. *NPJ Breast Cancer* 2025; 11: 5.
- [32] Allin KH, Nordestgaard BG, Flyger H and Bojesen SE. Elevated pre-treatment levels of plasma C-reactive protein are associated with poor prognosis after breast cancer: a cohort study. *Breast Cancer Res* 2011; 13: R55.
- [33] Madeddu C, Sanna E, Gramignano G, Tanca L, Cherchi MC, Mola B, Petrillo M and Macciò A. Correlation of leptin, proinflammatory cytokines and oxidative stress with tumor size and disease stage of endometrioid (type I) endometrial cancer and review of the underlying mechanisms. *Cancers (Basel)* 2022; 14: 268.
- [34] Lv D, Fei Y, Chen H, Wang J, Han W, Cui B, Feng Y, Zhang P and Chen J. Crosstalk between T lymphocyte and extracellular matrix in tumor microenvironment. *Front Immunol* 2024; 15: 1340702.